

In-Situ Deposition, Optical Characterization and Bandgap Shift of AgO Thin Films

Ifeanyichukwu Chinedu Amaechi

Department of physics and Astronomy, University of Nigeria, Nsukka, Enugu State, Nigeria

†Corresponding author: ifeanyichukwuonline@yahoo.com

Abstract

Porous and specularly reflective films of inorganic silver oxide (AgO) with thickness ranging from 275-435nm have been deposited by chemical bath (CBD) in a mixed solution of silver nitrate AgNO_3 and precursor of triethanolamine (TEA) maintained at a temperature of 318K. Surface morphology of the films was characterized by scanning electron microscopy (SEM). Optical and structural studies were performed to find the optical attenuation, some solid state properties and crystallographic structure for the individual films. High quality films with low transmittance $< 11.50\%$ in the visible and near infrared (NIR) region are obtained. Direct optical bandgap for the films lies in the range 1.5-1.7eV, whereas the refractive index developed peak in the dispersion region near 450nm. X-ray diffraction study indicates that the films composed of polycrystalline AgO with cubic structure belonging to the space group, $\text{fm}\bar{3}\text{m}$.

Keywords: Inorganic silver oxide, Triethanolamine (TEA), X-ray diffraction, Transmittance.

1. Introduction

Inorganic silver oxide (AgO) semiconductor films are known to exhibit *p*-type semiconductivity with a bandgap in the range 1.20-1.50 eV [1]. Despite its extensive use in photography and batteries (as an electrode) [2], the recent interest has culminated in its potential use as optical memories. Silver is known to show a tendency to non-continuous nucleation characterized by formation of islands in the early stage of the growth [3]. This is because it is rather difficult to reach the Stranski-Krastanov growth mode which is mandatory for obtaining smooth and continuous thin film.

Growth mechanism of thin metal film has been a little complex and the mode depends mainly on the wetting relation between the deposited material and the substrate. However, wetting is a function of adhesion energy and free energy of the metal and noble metals are not exception since they exhibit low adhesion energy to most oxides, which is caused by weak chemical bonding. Ag-O system, including Ag_2O , AgO, Ag_3O_4 and Ag_2O_3 , constitute a fascinating group of inorganic materials [4]. Silver oxides crystallize out in various types of crystal structures, leading to a variety of interesting physiochemical properties such as catalytic, electrochemical, electronic and optical properties [5]. Again, this inorganic metal oxide semiconductor has favored promising applications as a catalyst for ethylene and methanol oxidation [6,7], as a sensor for the detection of carbon monoxide and ammonia [8-11], as photovoltaic materials [12-14], as important components in optical memories [15] and plasmon photonic devices [16] or as active cathodic materials in silver oxide/zinc alkaline batteries [17,18].

In view of these fascinating applications, a variety of techniques had been employed in the synthesis of silver oxide: Banerjee et al [19] reported quantum confinement effects in heat-treated silver oxide nanoparticles. Barik et al [20] showed that rate of evaporation appears to control the nature of conduction for AgO thin films prepared by reactive electron beam evaporation. Silver doped indium oxide (IO) thin films have very interesting observations in electrical properties with varying oxygen stoichiometry in the film as reported by Asbalter and Subrahmanyam [21]. The report of Hou et al [22] centers on theoretical study of the fractal structure in silver oxide thin films. One of the recent reports shows that nanoclusters of AgO result to fluorescent phenomenon (after subjecting the film to 515nm irradiation) which maybe used in optic data storage [23].

In this investigation, deposition time effect, optoelectronic properties and bandgap shift of the inorganic silver oxide thin films prepared at 318K by chemical bath technique is reported.

2. Experimental details

The solution growth of AgO films employing CBD technique does not require a complex set-up or equipment and it is based on a hydrolytic decomposition of silver triethanolamine (TEA) complex formed in aqueous solution. At ambient temperature, the deposition rate appears to be retarded and as such an average temperature of 318K was maintained to ensure production of uniform and quality films. The substrates used are bare non-conducting quartz substrates. Prior to deposition, the quartz substrates were first cleaned by acetone, for eliminating any greasy track, then with soap and abundantly rinsed with distilled water. Finally, they were dried

by an oxygen flow.

AgO films were prepared using aqueous solution of silver nitrate (1.2M). Approximately 1.0g of solid metal nitrate was dissolved in 5 mL of bi-distilled water. Subsequently triethanolamine (TEA) was added drop-wise with constant stirring until the disappearance of brownish coloration. The chemistry of dissolution is such that the precipitate of AgOH upon constant stirring dissolves completely in appreciable quantity of TEA. The pyrex beaker content was made up to a volume of 80 mL by addition of bi-distilled water. With the help of Teflon holders, the degreased quartz substrates were immersed vertically in the prepared solution maintained at 318K on a hot plate. In 45 min, the nucleation of the metal oxide film has been initiated although the quantity is not good. Finally, after 90 min, the films were removed from the bath, rinsed with bi-distilledwater, drip-dried in air and then stored in vacuum desiccator.

The two dimensional surface topography of the as-deposited silve oxide films were observed with a scanning electron microscope (SEM, JEOL JSM-6400F). The structural analysis of the films were examined by x-ray diffraction (XRD) using X'pert Philips – MPD X-ray diffractometer with 40 mA, 45 kV CuK α radiation, $\lambda = 0.15406$ nm. The samples were scanned from 20 to 80 degrees in 0.02 degrees with a scan rate of 1.2 min⁻¹. Rietveld analyses were carried out on the samples to estimate the unit cell parameters, space group and symmetry. The thickness of AgO films was measured by commonly used weight difference method using a sensitive microbalance:

$$t = \frac{\Delta m}{\rho A} \quad (1)$$

where $\rho = 7.44\text{g/cm}^3$ for AgO and 10.5g/cm^3 for Ag [24] and A is the cross-sectional area.

Optical absorption measurements were taken at ambient temperature in the wavelength range 300 – 1100 nm, using Cary 5E UV-Vis-NIR spectrophotometer with plane glass substrate as reference.

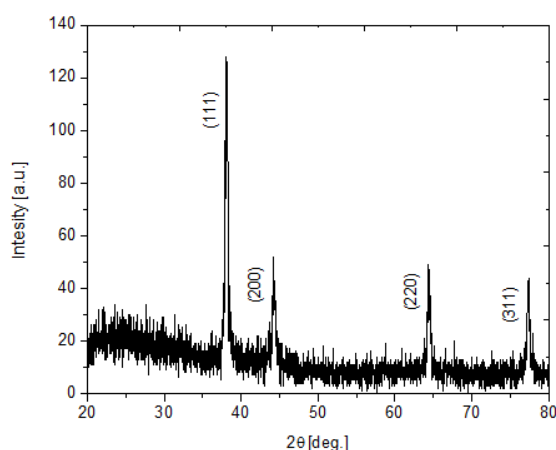


Fig. 1: X-ray diffraction pattern of inorganic AgO thin films deposited from precursor of triethanolamine solution.

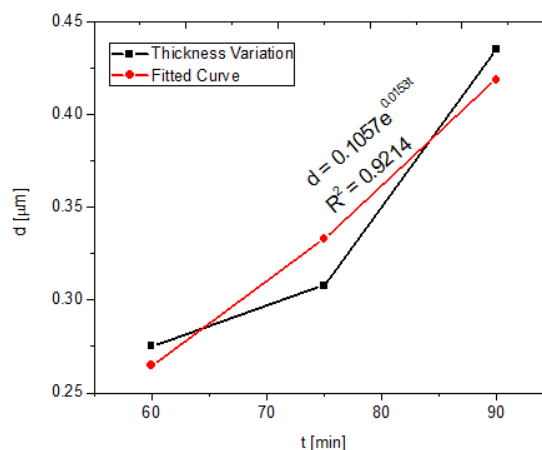


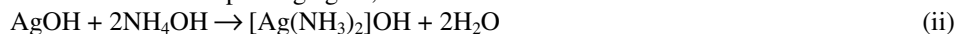
Fig. 2: Thickness dependence of AgO films on deposition time with relative exponential increment in plot.

3. Results and discussion

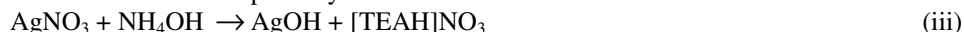
The chemistry of reaction for the deposition of silver oxide films is dependent on the complexing agent. Consider the complexing of silver ion by ammonium hydroxide, NH₄OH according to the following reaction:



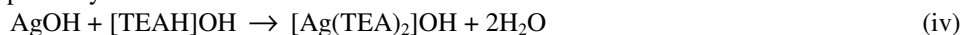
In the event that the complexing agent, NH₄OH is in excess then



Based on these simple physico-chemical reactions, we suggest that the cationic silver in triethanolamine, TEA assumes the same reaction pathway.



and probably in excess TEA



The equations of reaction above predict that silver triethanolamine complex undergoes a hydrolytic decomposition which entirely depends on the experimental conditions; either Ag or AgO is coated onto the substrate. Since the final product depends on the amount of TEA in solution and decomposition mechanism of

silver triethanolamine (Ag-TEA) complex is somewhat incoherent, we establish that Ag films are formed in sufficient amount of TEA otherwise AgO films follow in the presence of drops of TEA.

Fig.1 shows the X-rays diffraction pattern of the as-deposited AgO films. The observed diffraction peaks were compared with standard JCPDS-ICPD diffraction patterns from PDF-2 sets 1-43 database. As-deposited films are polycrystalline cubic phase with a major (111) reflection and three weak reflections characteristic of (200), (220) and (311) planes of AgO. The crystallite size was estimated from the full width at half maximum (FWHM) of the X-ray diffraction liner. The broadening of the FWHM is inversely proportional to the average crystallite size (D) as predicted by the well-known Scherrer's formular [24]:

$$D = \frac{k\lambda}{\beta \cos \theta} \quad (2)$$

where β is the observed angular width at half maximum intensity of the peak with $\beta^2 = \beta'^2 - \beta_0^2$, where β' is the measured line width at half maximum and β_0 is the instrumental broadening [24], $\beta_0 = 0.217^\circ$ with the apparatus used. k is the dimensionless number which is 0.89, λ is the wavelength of X-ray radiation used (0.15406 nm for CuK α), θ is the diffraction angle.

The value of crystallite size estimated from the most intense peak was 0.68 nm. The lattice constant and inter-planar spacing was calculated following the Bragg's law [25] assuming a cubic phase:

$$\frac{1}{d_{hkl}} = \frac{2 \sin \theta}{\lambda} = \frac{(h^2 + k^2 + l^2)^{1/2}}{a} \quad (3)$$

where d_{hkl} is the inter-planar spacing and λ is the wavelength of X-ray wavelength of CuK α radiation. Table 1 shows the consistency in calculated and JCPDS data for inter-planar spacing and lattice constant of AgO thin films.

Table 1: Inter-planar spacing and lattice constant deduced from XRD study of AgO thin films.

<i>h k l</i>	<i>As-deposited</i>	<i>JCPDS data</i>
(111)		
2 θ ($^\circ$)	38.117	38.115
d_{hkl} (nm)	0.23590	0.235917
(200)		
2 θ ($^\circ$)	44.279	44.299
d_{hkl} (nm)	0.20440	0.20431
(220)		
2 θ ($^\circ$)	64.428	64.443
d_{hkl} (nm)	0.14450	0.144469
(311)		
2 θ ($^\circ$)	77.475	77.397
d_{hkl} (nm)	0.12310	0.123204
a (nm)	0.40859	0.40862
Vol (\AA^3)	68.212	68.227

Fig. 2 shows the dependence of AgO film thickness upon deposition time. The red line in the plot represents the fitted curve which yields relatively an exponential increase given by the equation $d = 0.1057e^{0.0153t}$; where d is the film thickness (μm) and t is time in (minutes).The equation would be used to interpolate and predict film thickness of AgO at any other time depending on its application.

The SEM photographs of these deposited films shown in fig.3a-c corroborate these results. It can be seen that the morphology of the films depends more on deposition time than quantity of TEA added. Despite the variation in dip time, they all appear porous, highly inhomogenous and randomly shaped grains distributed onto a very smooth surface area without holes or cracks generated. The average grains size is of a few units of microns which is in good agreement with the XRD study.

The optical absorption studies and possible electronic transitions of inorganic AgO thin films were determined from the recorded transmission spectra. Fig.4 shows the spectral variation of transmission spectra of AgO thin films with different dip time in the wavelength range 300-1100nm. The transmission in the absence of interference fringes of a thin film deposited on a perfectly smooth substrate is given by [26,27].

$$T = \frac{(I - R)^2 e^{-at}}{I - R^2 e^{-2at}} \quad (4)$$

$$R = \frac{(n-1)^2 + k^2}{(n+1)^2 + k^2} \quad (5)$$

where $\alpha = \frac{4\pi k}{\lambda}$ is the absorption coefficient. By using these relations, n and k can be determined from the measurement of T and R using suitable computer programs. Otherwise the aforementioned quantities may be easily calculated in terms of the components of complex dielectric function as follows [28]:

$$n(w) = \left[\frac{\epsilon_1(w)}{2} + \frac{\sqrt{\epsilon_1(w)^2 + \epsilon_2(w)^2}}{2} \right]^{1/2} \quad (6)$$

$$k(w) = \left[\frac{\sqrt{\epsilon_1(w)^2 + \epsilon_2(w)^2} - \epsilon_1(w)}{2} \right]^{1/2} \quad (7)$$

where $\epsilon(w) = \epsilon_1(w) + i\epsilon_2(w)$, ϵ_1 and ϵ_2 represents real and imaginary part of dielectric function respectively. The maximum transmittance which is in the UV region at 325nm supports the argument that depending on thickness, the transmittance of AgO films in visible and near infra red portion of the *em* spectrum is either very small (for thinner films) or close to zero (for thicker films)[24]. Also, the plot of real part of dielectric constant ϵ_1 is shown in the inset of fig. 4. The dielectric for the films developed hump around 450nm in the visible region which decreased continuously towards the infrared region (IR).

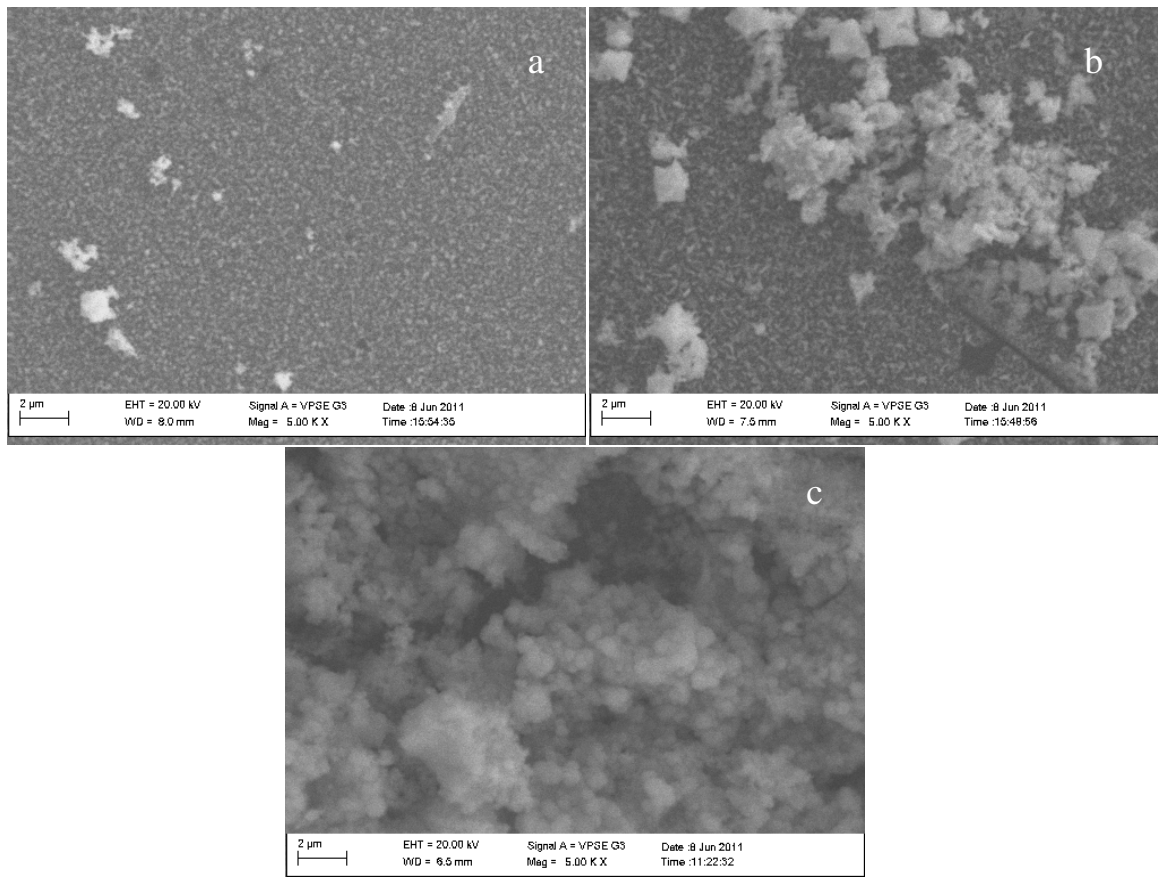


Fig. 3 a-c: The scanning electron microscopy of as-deposited AgO thin films at deposition times 1hr, 1.25hr and 1.75hr respectively

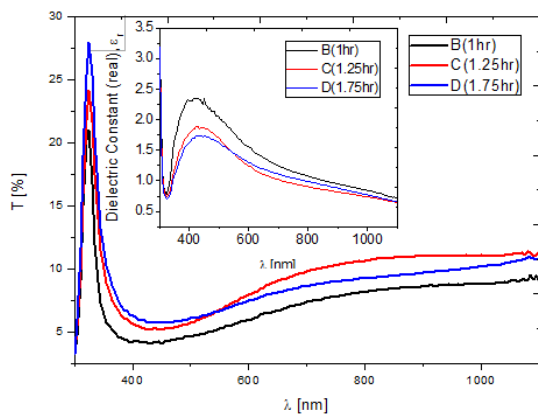


Fig. 4: The spectral transmittance of investigated AgO films deposited at 1hr, 1.25hr and 1.75hr respectively. Inset of fig.4 depicts the variation of dielectric constant (real) with wavelength.

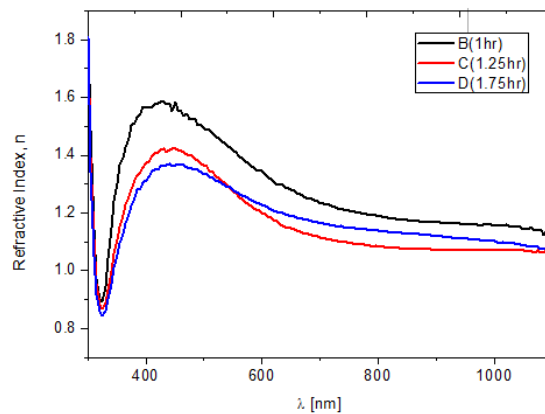


Fig. 5a: The plots of refractive index, n versus wavelength λ for AgO films

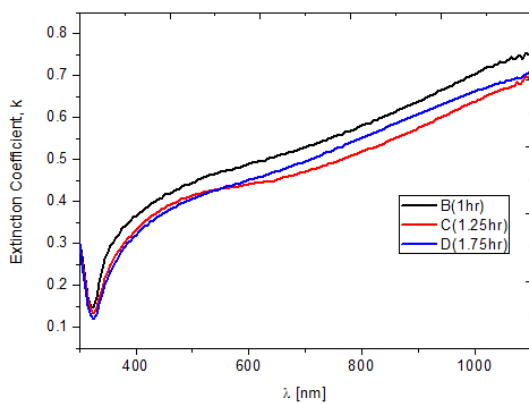


Fig. 5b: The plots of extinction coefficient k against wavelength λ for AgO films.

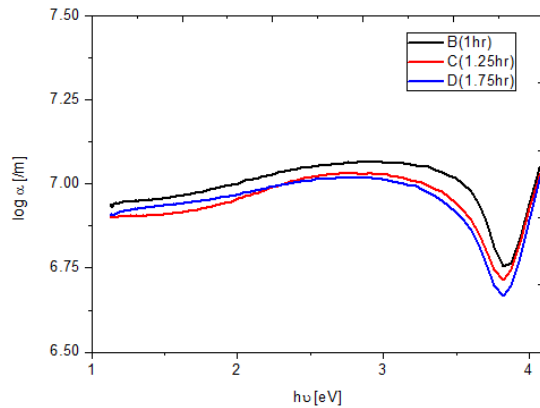


Fig. 6: The variation of absorption coefficient as a function of photon energy

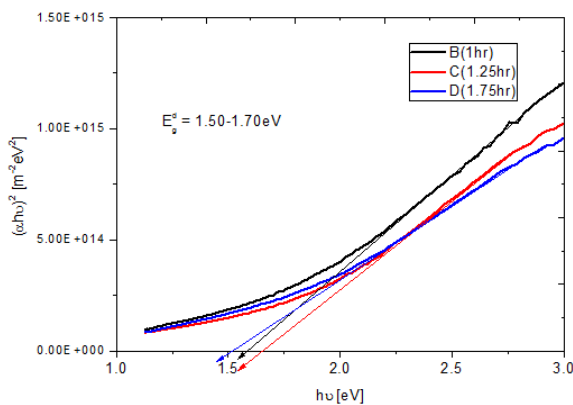


Fig. 7a: The plots of $(\alpha h\nu)^2$ versus $h\nu$ for silver oxide films

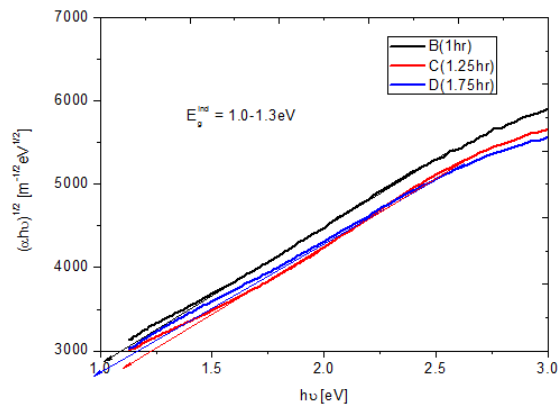


Fig. 7b: The plots of $(\alpha h\nu)^{1/2}$ versus $h\nu$ for silver oxide films

Fig. 5a and b show the spectral variation of the refractive index and extinction coefficient versus wavelength λ . It is obvious that slight variation was observed in both n and k with the film thickness. Therefore, it could be concluded that both n and k are dependent on the film thickness. Hence the refractive index developed peak in the dispersion region near 450nm. Thereafter, n tends to decrease with increasing wavelength. The nearly constant value of the refractive index, n_∞ at higher wavelengths ($\lambda \geq 1100\text{nm}$) was found to be 1.14, 1.06 and 1.08 for AgO films deposited at 1hr, 1.25hr and 1.75hr respectively. The optical constants are in strong agreement with that obtained by reactive DC magnetron sputtering for oxygen flow rate at 0.83sccm [2]. Also the extinction coefficient estimated at the aforementioned wavelength sequentially is 0.76, 0.69, and 0.71 respectively.

The absorption coefficient α was estimated using the mean value of the extinction coefficient k , at certain

wavelength, λ . The variation of absorption coefficient as a function of photon energy is displayed in fig. 6. It varies from $8.73 \times 10^6 \text{ m}^{-1}$ to $1.26 \times 10^7 \text{ m}^{-1}$ in the photon energy range 1.13-4.14 eV for the films. According to the well-known relation [29] of equation 8, optical bandgap was determined as follows:

$$\alpha = \frac{A(\hbar\nu - E_g)^\eta}{\hbar\nu} \quad (8)$$

where η determines the type of optical transition. For $\eta = 2$, the photon energy range 1.0-3.0 eV indicates an indirect transition, and $\eta = 0.5$ for photon energy range 1.0-3.0 eV indicates a direct transition. Fig.7a & b depict the plots of $(\alpha\hbar\nu)^2$ and $(\alpha\hbar\nu)^{1/2}$ against photon energy ($\hbar\nu$). For a case of almost linearity in plots, extrapolating energy bandgap along $\hbar\nu$ axis given that $(\alpha\hbar\nu)^2$ and $(\alpha\hbar\nu)^{1/2}$ equals zero yields 1.50-1.70 eV and 1.0-1.3 eV for the films respectively, which are slightly higher than the predicted direct optical bandgap for AgO [1]. The high energy bandgap has also been detected in electrodeposited silver (I) oxide semiconductor thin films by electrogenerated acid [13]. Such bandgap shift may be attributed to the preparative conditions subject to either drop-wise addition of TEA resulting to incomplete reaction rate or deposition time. By reason of equation 6 or 7, the real part of dielectric constant was determined. Inset of fig. 4 shows the spectral variation of real part of dielectric constant with wavelength. It is obvious from the plot that there is trough which exists in the UV region. However, the peak exhibited around 450nm decreased gradually from visible to NIR region. The dielectric constant for the films at higher wavelengths $\lambda \geq 1100\text{nm}$ lies in the range 0.5-1.0.

4. Conclusions

- Specularly films of AgO have been deposited by chemical bath containing triethanolamine TEA solution at 318k.
- Growth mechanism was not considered, however, chemistry of reaction suggests a hydrolytic decomposition of silver TEA ion complex.
- The optical absorption analysis of AgO thin films showed that both indirect and direct optical transitions exist in the photon energy 1.13- 4.14 eV.
- The refractive index has peak at 450nm in the dispersion region.
- The films have low transmittance <11.50% which almost vanishes for thicker films in the NIR region.
- We hope that the work can lead to acceptance of chemically deposited AgO as a prospective component in photography and optical memory applications.

References

- Fortin, E. & Weichman, F.L. (1964), "Photoconductivity in Ag_2O ", *Phys. Stat. Sol. (B)* **5**, 515-519.
- Barik, U.K., Srinivasan, S., Nagendra, C.L. & Subrahmanyam, A. (2003) "Electrical and Optical Properties of Reactive DC Magnetron Sputtered Silver Oxide Thin Films: Role of Oxygen", *Thin Solid Films* **429**, Elsevier, 129-134.
- Bul'ır, J., Novotný, M., Lynnykova, A. & Lan'cok, J. (2011), "Preparation of Nanostructured Ultrathin Silver Layer", *J. Nanophotonics* **5**, 51511-10.
- Pierson, J.F. & Rousselot, C. (2005), "Stability Of Reactively Sputtered Silver Oxide Films", *Surf. Coat. Technol.*, **200**, Elsevier, 276-279.
- Wei, W., Mao, X., Ortiz, L.A. & Sadoway, D.R. (2011) "Oriented Silver Oxide Nanostructures Synthesized Through a Template-Free Electrochemical Route", **21**, *J. Mater. Chem.*, 432-438.
- Weaver, J.F. & Hoflund G.B. (1994) "Surface Characterization Study of the Thermal Decomposition of AgO", *J. Phys. Chem.*, **98** 8519-8524.
- Bielmann, M., Schwaller, P., Ruffieux, P., Groning, O., Schlapbachand, L. & Groning, P. (2002), "Evidence for Mixed Valence AgO Investigated by Photoelectron Spectroscopy", *Phys. Rev. B: Condens. Matter Mater. Phys.*, **65**, 235431-36.
- Yamamoto, N., Tonomura, S., Matsuoka, T. & Tsubomura, H. (1981), "The Effect of Reducing Gases on the Conductivities of Metal Oxide Semiconductors", *Jpn. J. Appl. Phys.*, **20**, 721-726.
- Murray, B.J., Li, Q., Newberg, J.T., Menke, E.J., Hemminger, J.C. & Penner,R.M. (2005), "Shape- and Size-Selective Electrochemical Synthesis of Dispersed Silver(I) Oxide Colloids", *Nano Lett.*, **5**, 2319-24.
- Murray, B.J., Li, Q., Newberg, J.T., Menke, E.J., Hemminger, J.C. & Penner,R.M. (2005) "Silver oxide microwires: Electrodeposition and Observation of Reversible Resistance Modulation Upon Exposure to Ammonia Vapor", *Chem. Mater.*, **17**, 6611.
- Murray, B.J., Li, Q., Newberg, J.T., Walter, E.C., Hemminger, J.C. & Penner,R.M.(2005), "Reversible Resistance Modulation in Mesoscopic Silver Wires Induced by Exposure to Amine Vapor", *Anal. Chem.*, 2005, **77**, 5205.
- Tselepis, E. & Fortin, E. (1986), "Preparation And Photovoltaic Properties Of Anodically Grown Ag_2O Films", *J. Mater. Sci.*, **21**, 985-988.

- Ida, Y., Watase, S., Shinagawa, T., Watanabe, M., Chigane, M., Inaba, M., Tasaka, A. & Izaki, M. (2008), "Direct Electrodeposition of 1.46 eV Bandgap Silver (I) Oxide Semiconductor Films by Electrogenerated Acid", *Chem. Mater.*, **20**, 1254-1256.
- Breyfogle, B.E., Hung, C., Shumsky, M.G. & Switzer, J.A. (1996), "Electrodeposition of Silver (II) Oxide Films", *J. Electrochem. Soc.*, **143**, 2741.
- Her, Y., Lan, Y., Hsu, W. & Tsai, S.Y. (2004), "Effect Of Constituent Phases Of Reactively Sputtered Ag_x Film On Recording And Readout Mechanisms Of Super-Resolution Near-Field Structure Disk", *J. Appl. Phys.*, **96**, 1283.
- Tominaga, J. (2003), "The Application of Silver Oxide Thin Films to Plasmon Photonic Devices", *J. Phys.: Condens. Matter*, **15**, R1101.
- Parkhurst, W.A., Dallek, S. & Larrick, B.F. (1984) "Thermogravimetry - Evolved Gas Analysis of Silver Oxide Cathode Material", *J. Electrochem. Soc.*, **131**, 1739.
- Dallek, S., West, W.A. & Larrick, B.F. (1986), "Decomposition Kinetics of Ag_2O Cathode Material by Thermogravimetry", *J. Electrochem. Soc.*, **133**, 2451.
- Banerjee, S., Maity A.K. & Chakravorty, D. (2000), "Quantum Confinement Effect In Heat Treated Silver Oxide Nanoparticles", *J. Appl. Phys.*, **87**, 8541.
- Barik, U.K. & Subrahmanyam, A. (2000) in: Kumar, V. & Basu, P.K. (Eds.), Proceedings of 11th International Workshop on Physics of Semiconductor Devices, New Delhi, India, Dec 11–15, p.1271.
- Asbalter, J. & Subrahmanyam, A. (2000), "*p*-type Transparent Conducting In_2O_3 - Ag_2O Thin Films Prepared by Reactive Electron Beam Evaporation Technique", *J. Vac. Sci Technol.*, **18** 1672-76.
- Hou, S.M., Ouyang, M., Chen, H.F., Liu, W.M., Xue, Z.Q., Wu, Q.D., Zhang, H.X., Gao, H.J. & Pang, S.J. (1998), "Fractal Structure in the Silver Oxide Thin Film", *Thin Solid Films*, **315**, Elsevier, 322.
- Peysner, L.A., Vinson, A.E., Bartko, A.P. & Dickson, R.M. (2001), "Photoactivated Fluorescence From Individual Silver Nanoclusters", *Science* **291**, 103-106.
- Kocareva, T., Grozdanov, I. & Pejova, B. (2001), "Ag and Ag_2O Thin Film Formation in Ag^+ -Triethanolamine Solutions", *Materials Letters* **47** 319-323.
- Klug, H.P., Alexander, L.E. (1974), "X-ray Diffraction Procedures for Polycrystalline and Amorphous Materials", Wiley, New York.
- Pankove, J.I. (1971), "Optical Processes in Semiconductors", Dove, New York, p.103.
- Sze, S.M. (1981), "Physics of Semiconductor Devices", Wiley, New York.
- Okoye, C.M.I. (2003) "First-principles Study of the Electronic and Optical Properties of Zincblende Zinc Selenide", *Physica B* **337**, Elsevier, 1–9.
- Moss, T.S. (1973), "Semiconductor Opto-Electronics", Butterworth, London, p. 48.

The IISTE is a pioneer in the Open-Access hosting service and academic event management. The aim of the firm is Accelerating Global Knowledge Sharing.

More information about the firm can be found on the homepage:

<http://www.iiste.org>

CALL FOR JOURNAL PAPERS

There are more than 30 peer-reviewed academic journals hosted under the hosting platform.

Prospective authors of journals can find the submission instruction on the following page: <http://www.iiste.org/journals/> All the journals articles are available online to the readers all over the world without financial, legal, or technical barriers other than those inseparable from gaining access to the internet itself. Paper version of the journals is also available upon request of readers and authors.

MORE RESOURCES

Book publication information: <http://www.iiste.org/book/>

Academic conference: <http://www.iiste.org/conference/upcoming-conferences-call-for-paper/>

IISTE Knowledge Sharing Partners

EBSCO, Index Copernicus, Ulrich's Periodicals Directory, JournalTOCS, PKP Open Archives Harvester, Bielefeld Academic Search Engine, Elektronische Zeitschriftenbibliothek EZB, Open J-Gate, OCLC WorldCat, Universe Digital Library, NewJour, Google Scholar

